# Earths-field-NMR Remote

**Physikalisches Fortgeschrittenenpraktikum at University of Constance**

Authors: Philipp Gebauer, Simon Keegan and Marc Neumann

Tutors: Narinder Narinder and Matthias Falk

Execution on 9th of July 2020 and ???

## Abstract

The aim of this paper is to show the principals of an EFNMR measurement and to discuss its results.
The first part of the experiment is about the basic principal of EFNMR measurements. Therefore the noise level is taken to account and is identifeid to be 7.5 $\mu$V for our setup. The analysis of the $B_1$ coil results in a capacity of 13.8 nF for the LCR circuit in order to tune the circuit to the lamor frequency of 1841.4 Hz. To obtain a sharp peak in the spectrum for the measured hydrogen signal the system was tuned to following values: shimming values $x = 10.11$ mA, $y = 20.88$ mA, $z = -20.07$ mA; $B_1$ pulse duration 1.35 ms; capacity 13.8 nF. The relaxation time measurements in the polarizing field results in values for $T_{1,p}$ of 2912.8800(48) ms. The relaxation time measurements in the earths magnetic field results in values for $T_{1,e}$ of 2753.0500(12) ms. The measurements of $T_2$ results in values of 2691(12) ms with single *Hahn* echos and 2317.760 00(62) ms with the use of 30 echos in a CPMG.

All authors have worked equally on all parts of this paper and used no other sources than listed in the bibliography.

## Contents

# 1 Introduction

Earths field nuclear magnetic resonance is a widely used method in the quality management or in medical technology to gain knowledge of a materials properties. Therefore the magnetic moment of spins is taken into account.
Due to the external magnetic field of the earth $B_0$ (sometimes refered to $B_e$) the spins of hydrogen (spin quantum number: $I = \frac{1}{2}$) align either parallel or antiparallel to this magnetic field. If the spins are aligned parallel or antiparallel can be calculated using the *Boltzmann* statistics. Therefore the temperature and the surrounding magnetic field $B_0$ is taken into account. Each spin precesses around this surrounding magnetic field $B_0$ (along z-axis), most often in the spin up direction, because it is energetically more favorable. This precession evokes a component of the spins in the transversal plane. However, since the phase of the precession is random the net magentisation is aligned along the z-axis. By changing the properties of the surrounding magnetc field the bulk magentisation vector can be manipulated. In order to do so an alternating electro magnetic field pulse is applied. The frequency of this magnetc field ($B_1$ coil) is in the radio frequency (RF)magnitude for large $B_0$ and for low $B_0$ it is in the ultra low frequency (ULF). Since we use the earths magnetic field as $B_0$ for our measurements, the frequency is in the ULF magnitude. When the frequency of this magnetic field pulse is chosen right at the lamor frequency of the sample, then the transitions between the energy levels between spin up and down happen more likely and therefore a phase coherence of the spins occurs. The applied pulse results in changing the spins direction by a tipping angle $\Theta$. The precession of the spins can measured in the transversal plane by a coil ($B_1$ coil) which is aligned orthogonal to the earths magentic field. The $B_1$ coil is therefore the exciting and detecting coil and therefore the heart of our measurements.
The first part of this experiment is about the basics of ENMR. At first we have a look at the noise that is dependent on surrounding metal objects. Then we analyse the $B_1$ coil by changing the capacity of the LCR circuit of it. The nex step is the optimization and characterisation of a free induction decay (FID) of a water sample. The aim of this chapter ist to measure a sharp peak at the lamor frequency of the hydrogen in the water. When this is done the longitudinal relaxation time $T_1$ and the transversal relaxation time are measured and discussed.

# 2 Setup

This chapter is about the setup and execution process of this experiment. To understand which part of the experiment has what use, it is necessary to have a look at the components of the setup.

Figure 2.1 shows the different coils which are necessary for the EFNMR measurement. The innerst coil $B_1$ coil is the excite and collect coil which is described in the previous chapter. The outer coil is to prepolarize the sample. This is necessary to obtain a stronger signal. By applying a strong magnetic field orthogonal to the earths magnetic field the spins align in the direction of the prepolarizing pulse and provides a bulk polarized nuclear magnetization across the sample. The middle coil is the gradient coil. This coil erases the inhomogenious magnetic field which always occurs for different uncertainty reasons. This coil is also used for the 2D imaging of the probe by adjusting the components of the magnetic field. Via the computer program *Prospa* and the spectrometer the currents of the coil can be adjust and the induced signals can be measured.

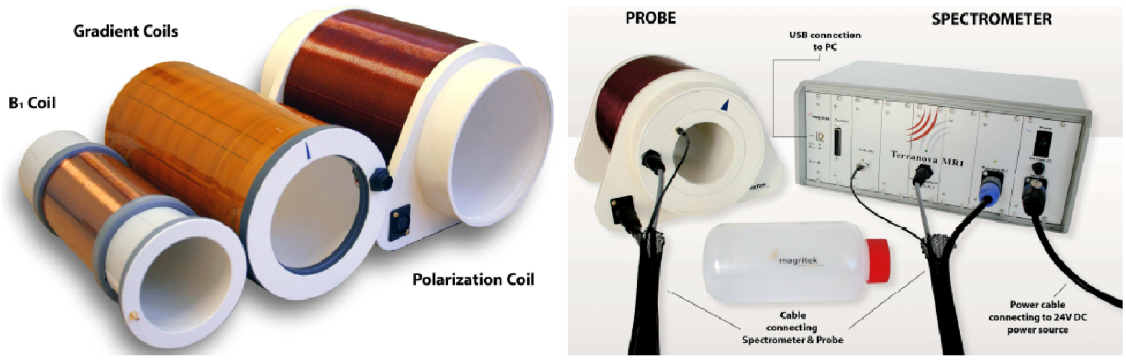


**Figure 2.1:** Setup of the *Terranova-MRI EFNMR*. On the left handside the coils $B_1$ (excite and collect coil), gradient coil (homogenious magnetic field and 2D scanning coil) and the prepolarizing coil $B_p$ are seen. The right hand side shows the water sample which has been used and the spectrometer which adjusts the right signals to the coils. [Mor01]

# 3 Noisemeasurement

The first step in the EFNMR Remote experiment is to measure the external noise. The external noise depends on the location where the setup is placed, the orientation of the probe and by surrounding metal objects e.g. a metal desk. To detect this external noise, a measurement without an NMR signal is provided. The time domain noise signal is shwon in figure 3.1. It is clearly visible that the noise is centered around $0\,\mu$V. To gain knowledge about the noise level, the computer calculates the root-mean-square (RMS). This means that it calculates the square of each data point, than sum up all squared values up, calculates the average and than applies a square root. With this method the noise level can be calulated. In this case it is $7.5\,\mu$V. This is an ecceptable noise value, because any value below $10\,\mu$V is good enough to provide good NMR data.

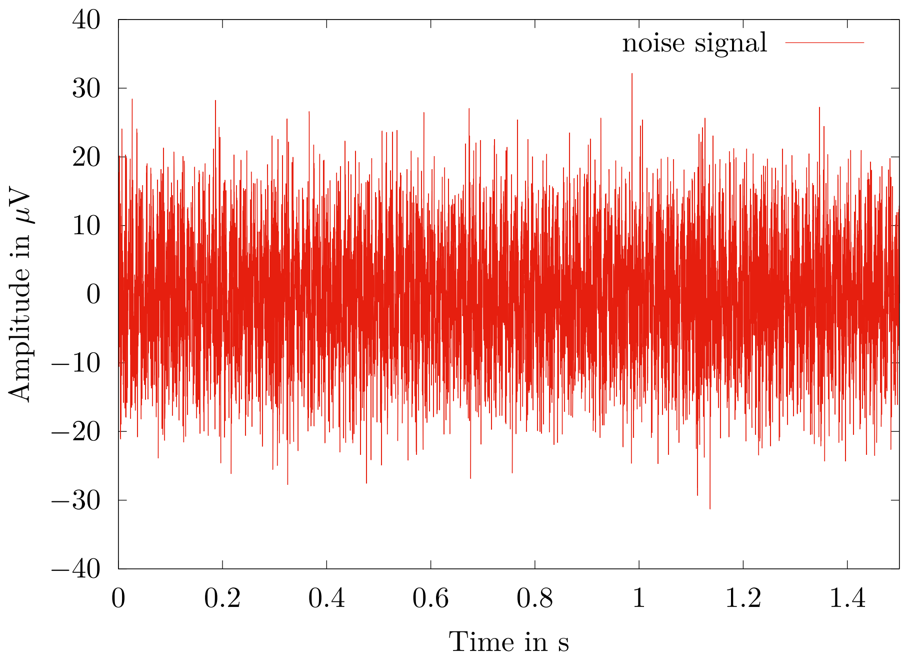


**Figure 3.1:** Noise signal taken by the $B_1$ coil. The noise value of this noise is $7.5\,\mu$V.

Figure 3.2 shows the frequency domain noise. This means that the time domain is fourier transformed into the frequency domain. This method is one of the basic principles we use in this experiment to make research about the properties of the measured signals. The frequency domain noise shows very specific sharp peaks every 50 Hz. To be more specific the peaks in the middle of every hundred Hz steps are way higher than those at 1400 Hz, 1500 Hz and so on. This results of the frequency in the power grid which is 50 Hz in

Germany. wieso sind die geraden kleiner??? Steckdose erklärt eig nur peak bei 50hz und nicht die alle 50 hz Despite all sharp peaks there is also a slight increase of the amplitude around 1850(1000) $\frac{\mu V}{Hz}$ visible. This is explicable by the resonance frequency of instrument and its sensitvity around the lamorfrequency (1841.4 Hz for water in Germany in July 2020). Nearby the lamorfrequency all our following measurements will be done that is why the instrument sensitvity is sharpend around this value.

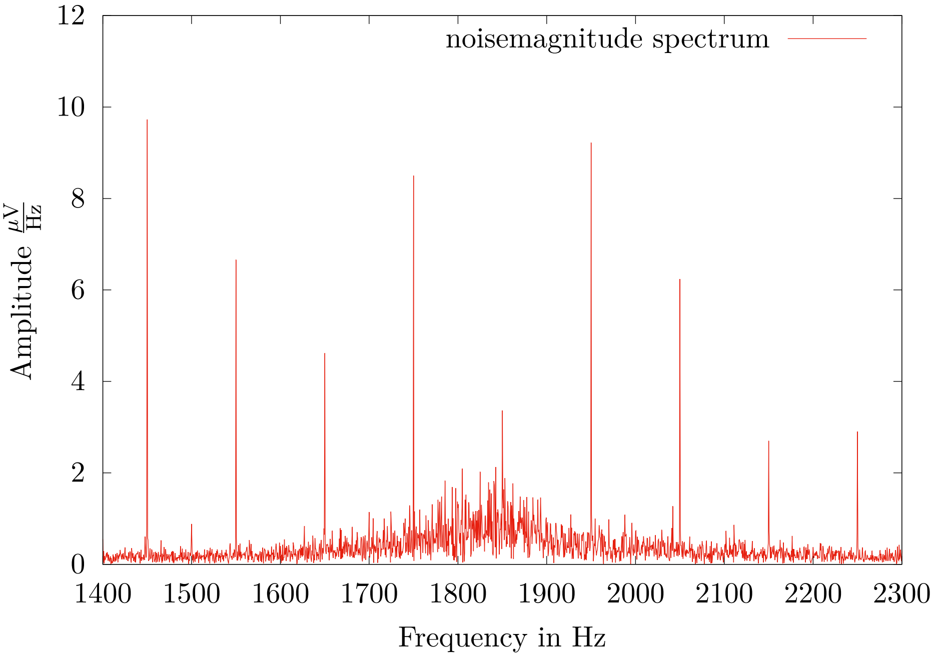


**Figure 3.2:** Fourie tranformed noise signal of the previous figure 3.1. Strong peaks every 50 Hz correspond to the frequency of the power grid in Germany. The slight increase of the amplitude around 1850(1000) $\frac{\mu V}{Hz}$ is explicable by the resonance frequency of instrument and its sensitvity around the lamorfrequency (1841.4 Hz for water in Germany in July 2020).

# 4 Coil Analysis

Now knowing that we have a acceptable noise value under 10 $\mu$V, we can analyse the coil. In order to do so we explain the general approach of NMR signals first. To measure a NMR signal a pulse and collect measurement has to be done. Therefore the $B_1$ coil (transmit and collect coil) has to apply a pulse. This pulse changes the spins direction out of its thermal equilibrium (along z-axes, due to the earths magnetic field $B_e$) into a direction with a component in the transversal plain. Therefore the $B_1$ coil collects a signal, because its aligned orthogonal to $B_e$. The transmit and collect procedure is based on Faraday's law of induction. Figure 4.1 exemplary shows such a collect signal by the $B_1$ coil. Every following measurement in this paper is based on the procedure of pulse and collect.

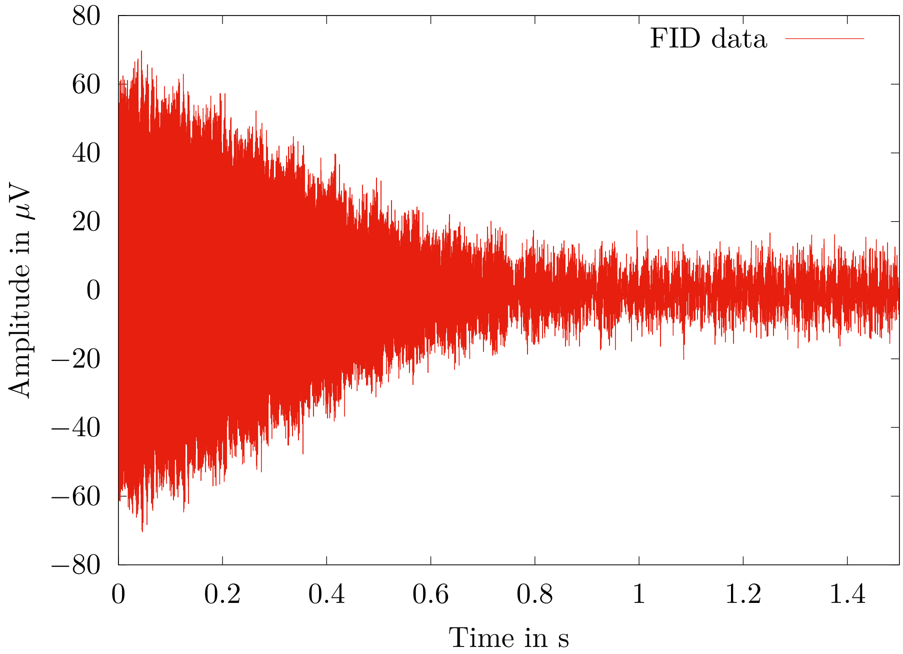


**Figure 4.1:** Example signal for a pulse and collect signal made by the $B_1$ coil. The example signal is taken from a FID signal.

Due to the fact that the $B_1$ coil is a tuned LCR circuit a resonance frequency exists, which can be caluclated by following formula:

$$\omega_{calc} = \frac{1}{\sqrt{L \cdot C}} \ . \tag{4.1}$$

To analyse the $B_1$ coil the resonance frequency versus the capacity is measured. Therefore the $B_1$ coil transmits a signal. Due to this signal the response of the coil can be measured. This signal is than fourie tranformed and the resonance frequency can be deduced from the frequency domain (maxmimum in the frequency domain). This procedure is repeated automatically by the computer programm "*Prospa*" for different capacities. By changing the capacity we can examen the best capacity in dependence of the lamor frequency. Figure 4.2 shows the measured and theoretically calculated resonance frequency (Equation 4.1; $L = 0.417\,\mathrm{H}$) in dependence of the capacity. The horizontal line represents the lamor frequency of 1841.4 Hz for water in Germany in July 2020. To gain this value the vertical component of the earths magnetic field ( 43 248.8 nTQuelle Marc) is multiplied to the gyromagnetic ration 42.577 $\frac{\mathrm{MHz}}{\mathrm{T}}$. Quelle Marc. The vertical line represents the correct capacity we should use for our measurement, due to the resonance frequency of the lamor frequency. In this case the correct capacity is 13.8 nF. For the calculated resonance frequency the correct capacity would be 17.9 nF. It is not deniable that the measured curve is not parallel to the measured resonance frequency. This probably has its cause in the not fix inductance $L$. Due to heating of the coil $L$ might change a little by increasing capacity and thus the calculated curve does not fit to the measured one.

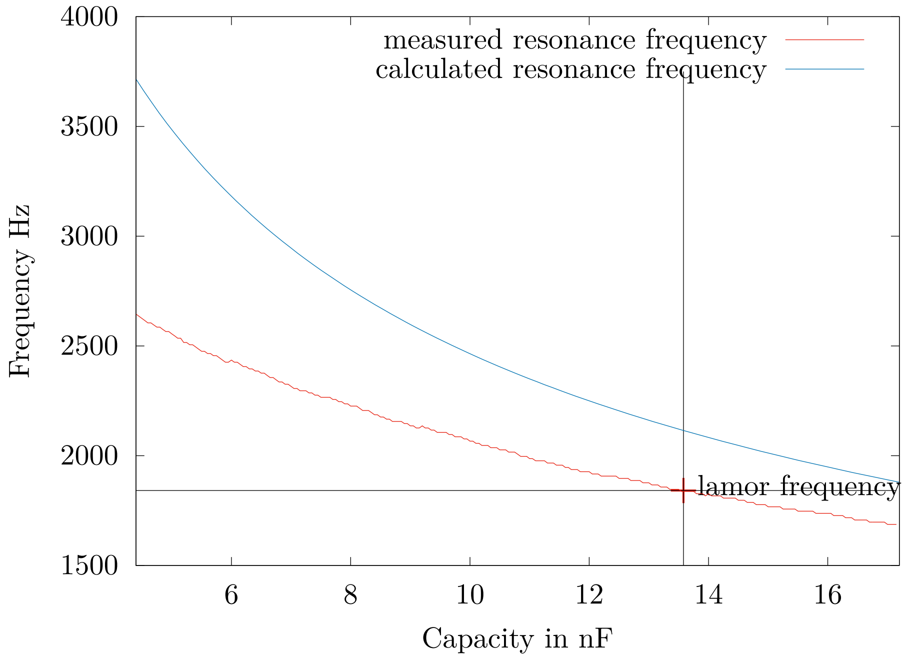


**Figure 4.2:** This figure shows the measured and calculated resonance frequencies for different capacities. The marked cross represents the lamor frequency of 1841.4 Hz for water in Germany in July 2020.

# 5 Optimization and Characterisation of FID in water sample

On of the main goals of this experiment is to measure a good FID of the water sample. In order to do so we first have to optimize our FID signal of the water probe.
First the inhomogenity of the magnetic field has to be cancelled. The process to make the magnetic field more homogenious is to *autoshimm* the components of the gradient coil. The computer programm does this automatically. So it deshimms the system step by step and checks if the output maximizes or minimizes. By checking many different

combinations it finds the best shimming values for the gradient coil. In our case they are:

$$x = 10.11\,\text{mA}$$
$$y = 20.88\,\text{mA}$$
$$z = -20.07\,\text{mA}\ .$$

That means with those shimming values the magnetic field in the setup is homogenious. The secon optimization step is to change the $B_1$ pulse duration. The longer the pulse duration is, the bigger is the angle of the flipping spins and thus the signal will get stronger (only counts for flipping angles till 90°). The best signal is obtained for an flipping angle of 90°, because with this angle the spins only have a component in the transversal plane and therefore the signal is maximized. If the pulse duration is too long, than the flipping angle is bigger than 90° and the spins get a horizontal component again and the signal will decrease again. When a flipping angle of 180° is reached the signal will be at its minimum. Afterwards the signal will raise again, because the horizontal component will increase again. Figure 5.1 shows this issue. The maxmimum at a pulse duration of 1.35 ms is clearly visible. This means that after apllying a $B_1$ pulse with a duration of 1.35 ms the spins are in the transversal plane and therefore the best signal is obtained.

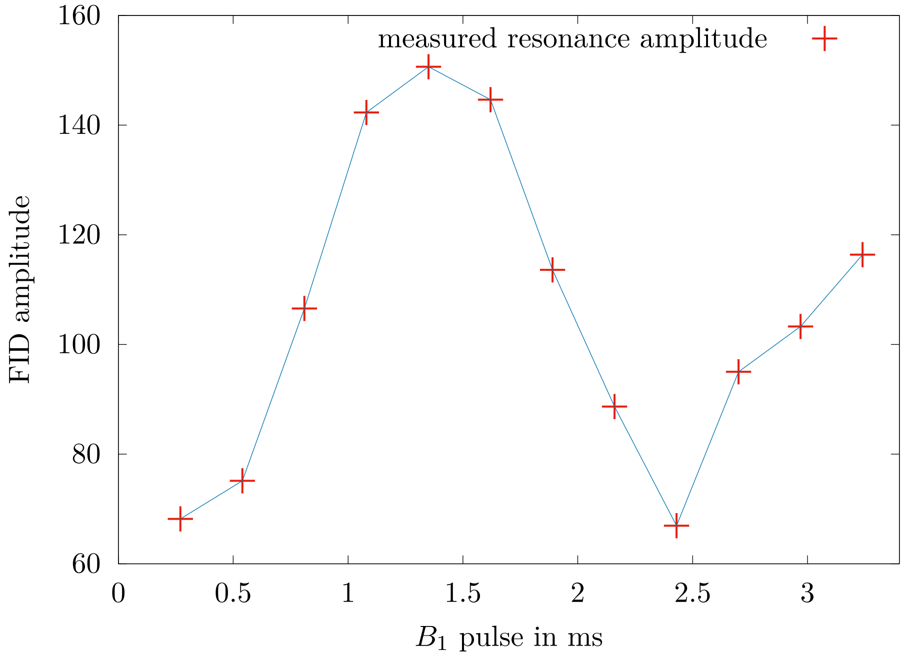


**Figure 5.1:** This figure shows which impact the $B_1$ pulse duration has to the ampitude of the FID. It is clearly visible that the duration has a maximum at 1.35 ms which is the duration for a 90° pulse.

Figure 5.2 exemplarily shows the correlation of the $B_1$ pulse duration and the signal which the coil detects. It is clearly visible that the amplitude is better for the pulse duration of 1.35 ms than for the pulse duration of 0.27 ms. The signal that was taken for the pulse duration of 0.27 ms is at the minimum of the figure 5.1 and therefore it is correct that the amplitude of the spectrum with the pulse duration of 1.35 ms is higher.

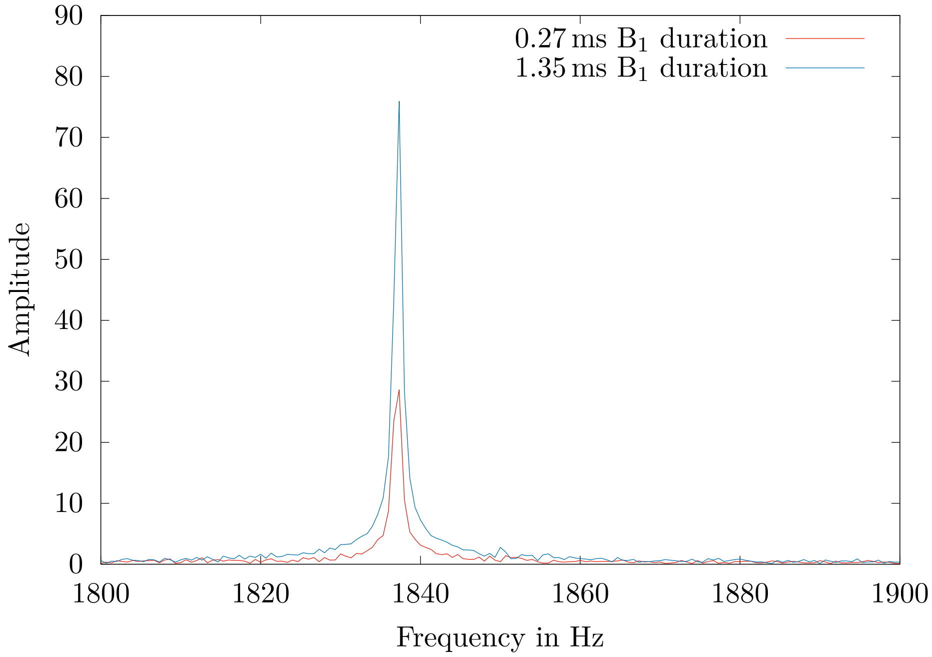


**Figure 5.2:** Example spectrum for two different $B_1$ pulse durations. The peak which is higher corresponds to the 1.35 ms duration pulse and represents the 90° pulse. This peak is high, because at this duration most of the spins are in the transversal plane and therfore the amplitude is maximal.

Now that the $B_1$ pulse duration is also optimized, we can have a closer look at the capacity of the LCR circuit of the $B_1$ coil again. First it is necessary to know that the $B_1$ pulse is applied by a *rectangular* function and the fourie transformation of a *rectangular* function is a *sinc* function. Therefore the fourie ransformed spectrum of the $B_1$ pulse signal is a *sinc* function. When we measure the signal shortly (acquisition delay: 2 ms) after the 90° pulse there shoud be a *sinc* function visible and indeed this is what we obtained (figure 5.3). In figure 5.3 there is also a really sharp peak visible. This is referd to the hydrogen signal. The hydrogen signal is independed of the applied capacity, but the $B_1$ pulse is, because the capacity changes the properties of the LCR-circuit of the $B_1$ coil. The best capacity is adjusted when the hydrogen signal is in the middle of the *sinc* function, because then the LC- circuit is tuned to the lamor frequency of the hydrogen signal. This is also visible by the amplitude of the spectrum in figure 5.3. The ampitude of the spectrum which was observed for a capacity of 13.8 nF is higher than for the ampitude of the spectrum which was observed for a capacity of 14.2 nF. As already explained before in the chapter 4 the capacity of 13.8 nF is indeed the best capacity in order to observe a maximized spectrum.

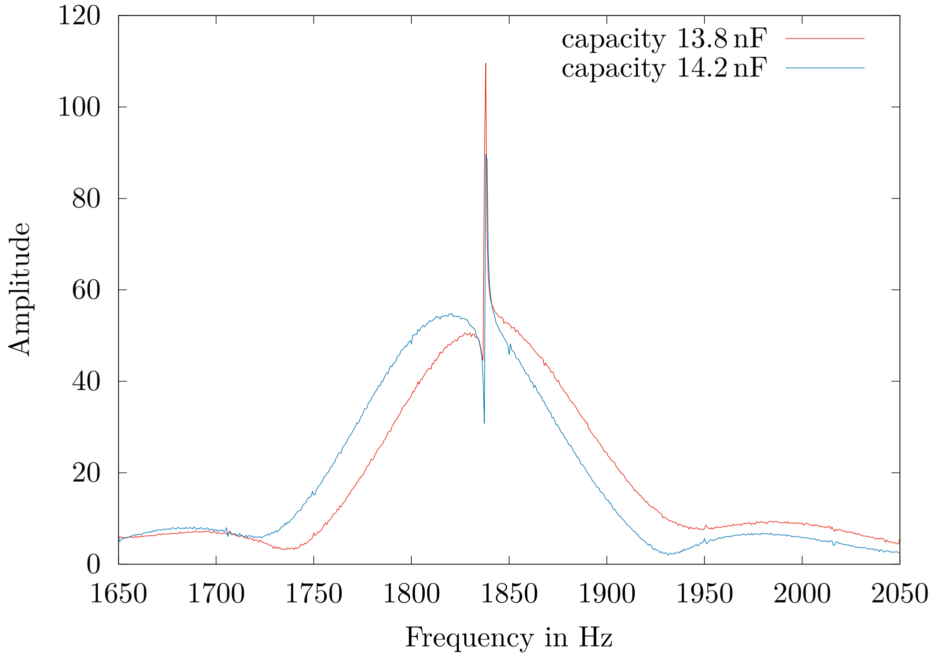


**Figure 5.3:** This figure shows the impact of the capacity in the LCR circuit of the $B_1$ coil. The *sinc* function comes from the fourie transformed $B_1$ pulse, which is rectangular. The peak at 1837.27(5) Hz is the peak from the hydrogen signal.

Now that the FID signal is optimized best we can start to characterize it. Therefore we measure a FID with a acquisition delay of 25 ms, because after this delay there are no effects from the rectangular applied $B_1$ pulse anymore (no *sinc* function in the spectrum). The figure 5.4 shows the observed spectrum and two different fit possibilities.
One option to fit a peak in a spectrum is by applying a *voigt*-profile ($V(x;\sigma,\gamma)$). This function is a convolution of the *Cauchy-Lorentz*- and *Gaussian*-distribution and is described by following formula:

$$V(x;\sigma,\gamma) = (G \star L)(x) = \int G(\tau)L(x-\tau)d\tau \tag{5.1}$$

$$G(x;\sigma) = \frac{exp\left(\frac{-x^2}{2\sigma^2}\right)}{\sigma\sqrt{2\pi}} \tag{5.2}$$

$$L(x;\gamma) = \frac{\gamma}{\pi\left(x^2+\gamma^2\right)} \quad . \tag{5.3}$$

$\sigma$ represents the standard deviation, $\gamma$ is half of the peak width at half height from the *Lorentz*-distribution and $x$ is the shift from the line center. In figure 5.4 the *voigt*-profile

(green) is fitted to the measured spectrum (red). The problem about this fit is that is not as sharp as the measured data. This might be, due to the fact that the measured spectrum does not have many data points especially around the maximum. Therefore the peak is really sharp and a correct fit with the *voigt*-profile is rather difficult. Therefore a second fit function has been apllied. This time only the *Gaussian*-distribution. This fit function is better to calculate the width of the peak, due to the fact that it easier to fit to this narrow peak. The full width of the peak at have maximum (FWHM) is calculated by the applied *Gaussian*-fit and is 1.180(40000) Hz.
The amplitude of the peak is 73.85 according to the *Gaussian*-fit and is in comparison to the amplitude of the noise measurement (magnitude 1) in figure 3.2 high. That means that the peak must come from the hydrogen signal is barely disturbed by any noise.
The disadvantage of the *Gaussian*-fit is that area under the curve does not equal the measured one, especially around 1836 Hz and 1839 Hz. Therefore the discussion about the integral under the measured curve will just be qualitative and will be done in the chapter 7.
real and imaginary signal -> explain it
signal to noise ratio: what to do? -> magnitude, which unit is the amplitude, tutor will send us an email, try back fouriertransform (only keep real values)

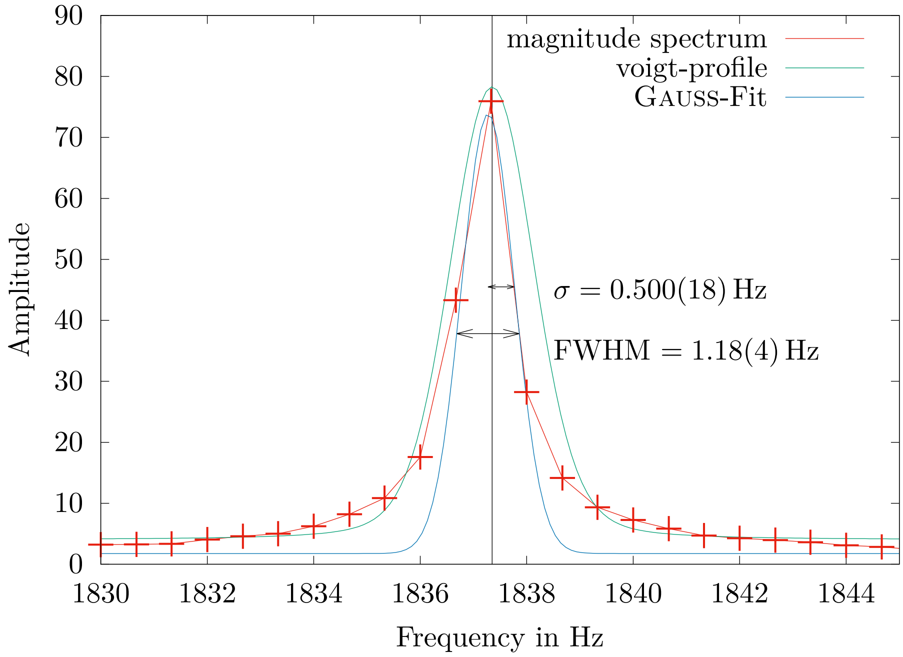


**Figure 5.4:** This figure shows the measured hydrogen signal after an acquisition delay of 25 ms and two possible ways to fit the peak. Due to a very short frequency range the peak looks very wide. Indeed it is actually very sharp. To fit the peak a *voigt*-profile and *Gaussian*-fit is used.

# 6 Longitudinal relaxation measurements T1

To measure the longitudinal spin lattice relaxation exist two possibilities. The first we want to have a closer look at is the measurement via $\tau_p$ (polarizing pulse duration). Therefore the computer program *Prospa* applies a polarizing pulse orthogonal to the earths magentic field. Due to this polarizing pulse the spins align in the transversal plain and form a bulk magnetisation. By time the magnetisation becomes stronger, therefore the signal becomes stronger. This relation is visualized in the figure 6.1.

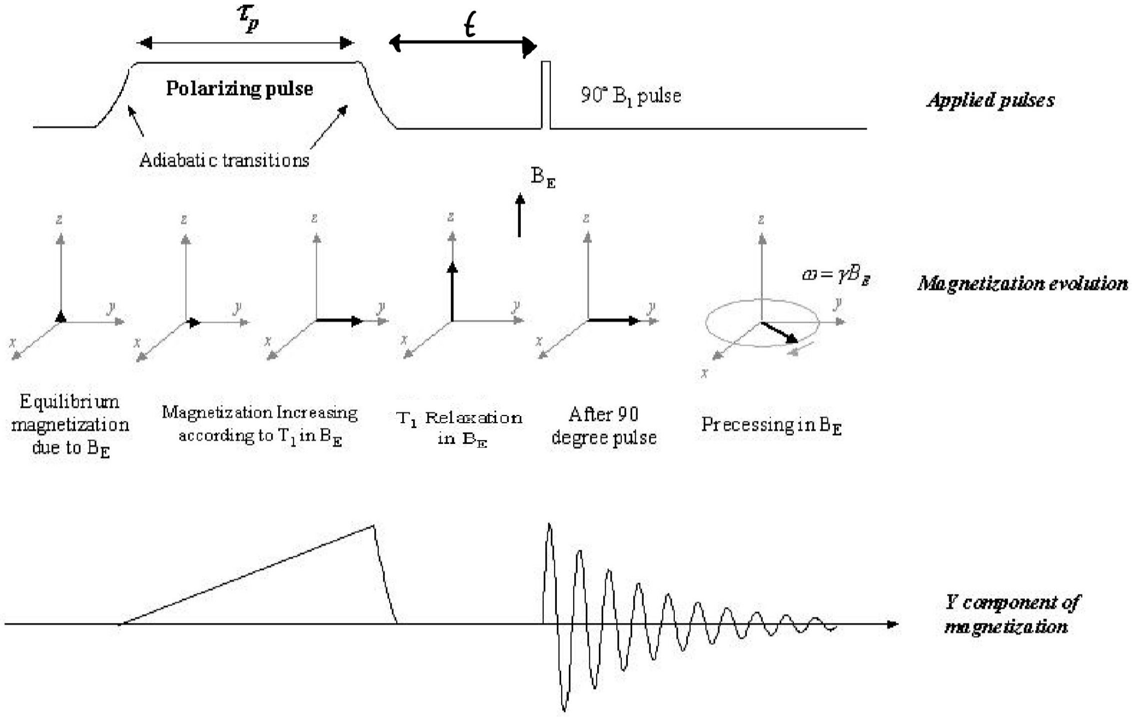


**Figure 6.1:** Sketch to show how $T_1$ can be measured. One way is by changing the polarizing pulse duration $\tau_p$ and the other way is by variy the time between the polarizing pulse and the 90° pulse. [Mor01]

Due to the increasing magnetisation it is possible to calculate the $T_{1,p}$ relaxation. In order to do so the magnetisation time is increased step by step from 500 ms to 4500 ms in step sizes of 500 ms and in each configuration the signal maximum is calculated of the fourie transformed spectrum. Figure 6.2 shows the attenuation of the signals normalized to the maximum peak $E_0$. The reason of that is that by applying a fit function as followed:

$$S(x) = S_0 \cdot [1 - exp(\frac{-x}{T_{1,p}})] \ , \tag{6.1}$$

it is possible to calculate the relaxation time $T_{1,p}$. The exponential decay is a result of loss of phase coherence between the spins and will be used for every measurement of spin relaxation. In this case $T_{1,p}$ is 2912.8800(48) ms.

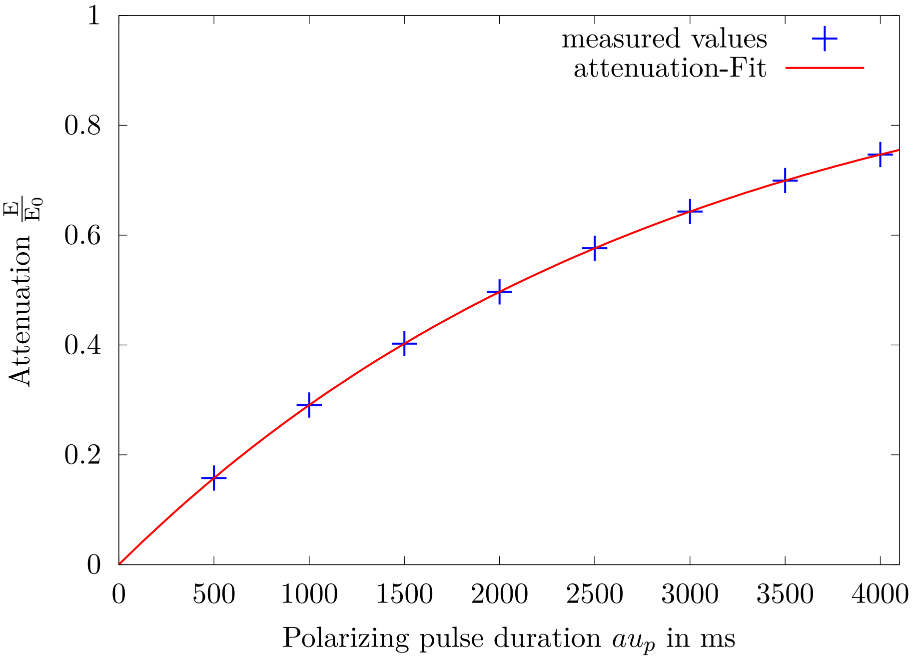


**Figure 6.2:** $T_{1,p}$ measurement by variy $\tau_p$ and see how the attenuation $\frac{E}{E_0}$ evolves. The provided exponential fit results in a value for $T_{1,p}$ of 2912.8800(48) ms.

The second option is to calculate the spin lattice relaxation via the earths magneitc field $B_e$. In this case the index will be $e$ for the spin lattice relaxation. The procedure in this case is to change the time $t$ (pre-90 minimum delay) between the polarizing pulse ends and the 90° pulse beginns. This relation is also visualized in the figure 6.1. The pre-90 minimum delay is chosen as 0 ms and the pre-90 delay step size 500 ms. For every configuration the signal maximum is calculated again of the fourie transformed spectrum. Figure 6.3 shows the attenuation of the signals normalized to the maximum peak $E_0$. This time the $T_{1,e}$ can be calculated by following fit function:

$$S(x) = S_0 \cdot exp(\frac{-x}{T_{1,e}}) \ . \tag{6.2}$$

For our case $T_{1,e}$ is 2753.0500(12) ms.
In both ways the uncertainty of the $T_1$ values are really small. This is the result of really good align values to the fit function. Nevertheless $T_{1,p}$ and $T_{1,e}$ are not consistent even though the uncertainty is considered. This might be, due to the fact that those to measurements are based on two different methods and there can always be differences in the setup genauer anschauen. Even though they are not consistent, the values for $T_{1,p}$

and $T_{1,e}$ have the same magnitude.

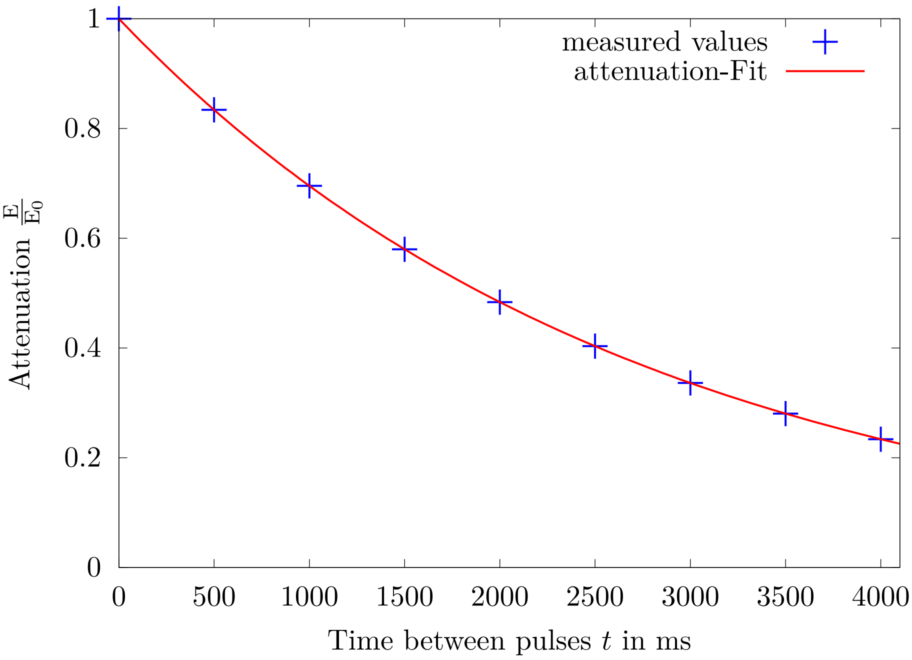


**Figure 6.3:** $T_{1,e}$ measurement by variy $t$ and see how the attenuation $\frac{E}{E_0}$ evolves. The provided exponential fit results in a value for $T_{1,e}$ of 2753.0500(12) ms.

# 7 Hahn echo

The other relaxionmeasurement is the $T_2$ measurement. In order to understand that, we first have to explain the *Hahn* echo and the principle of multiple echo sequences.
The principle of the *Hahn* echo is that an 90° pulse is applied and after a certain time $\tau$ a 180° pulse. The reason behind this method is that after the 90° pulse the spins are oriented in the transversal plane and start to precise around the earths magnetic field vector (z-axis). Due to spin-spin interaction (inhomogenious magnetic field accrues) the spins also interact with each other and therefore some spins have a higher lamor frequency and some have a smaller one. If an 180° pulse is applied after a certain time the spins will flip in the transversal plane and the slow precessing spins will be before the fast precessing spins again and when the fast precessing overtake the slow ones again the $B_1$ coil will de detect a signal again. The reason why the $B_1$ coil does not detect something while the slow and fast precessing spins are at different position is that they erase each other. If the spin-spin interaction is too weak than it also helps to deshimm the system along the

x-direction. This also makes the homogenious magnetic field inhomogenious and thus the spins will get different lamor frequencies according to there position.
Figure 7.1 exemplarily shows the *Hahn* echo for a shimming value of 4.95 mA along the x-axis (original value 10.11 mA). It is also possible to change the time between the 90° and 180° pulse. This would shift the peak to higher times in the timescale and due to loss effects the amplitude will shrink a little bit.

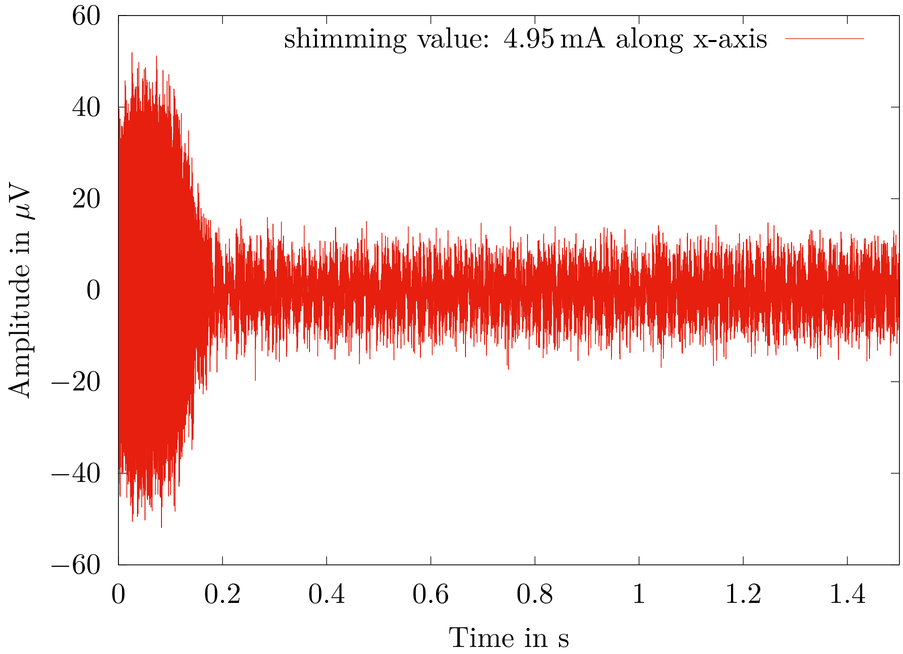


**Figure 7.1:** Example of a single *Hahn* echo for an echo time of 0 ms. The maximum of the echo is clearly visible. Due to relaxation after the maximum the signal after about 0.2 s is noise.

It is also possible to fourie transform the signal from figure 7.1. Figure 7.2 shows this for two different shimming values. The amplitude of the spectrum with the shimming value of 0 mA along the x-axis is clearly smaller than the amplitude of the spectrum with shimming value of 4.95 mA along the x-axis. This effect comes from the more inhomogenious magnetic field of the spectrum with the shimming value of 0 mA along the x-axis. A more inhomogenious magnetic field also means that the spins have more different lamor frequencies and thus the total intensity will shrink. The area under the spectrum should be independent from the inhomogeneity, because in total the magnetisation has to be the same. Only the distribution is different. This effect is also really good visible in the figure 7.2. This time it is not possible to find a good fitting function. Therefore this discussion is more qualitativ as mentioned before in chapter 5. The reason why there is no good fitting function is that there are a lot of random peaks in the spectrum and the more peaks there are the more difficult it is to find a good fitting function. Another thing which makes it rather hard is that the frequency steps are not very small and thus there are not many datapoints to make a good fit. This was also a problem in chapter 5 as mentioned before.

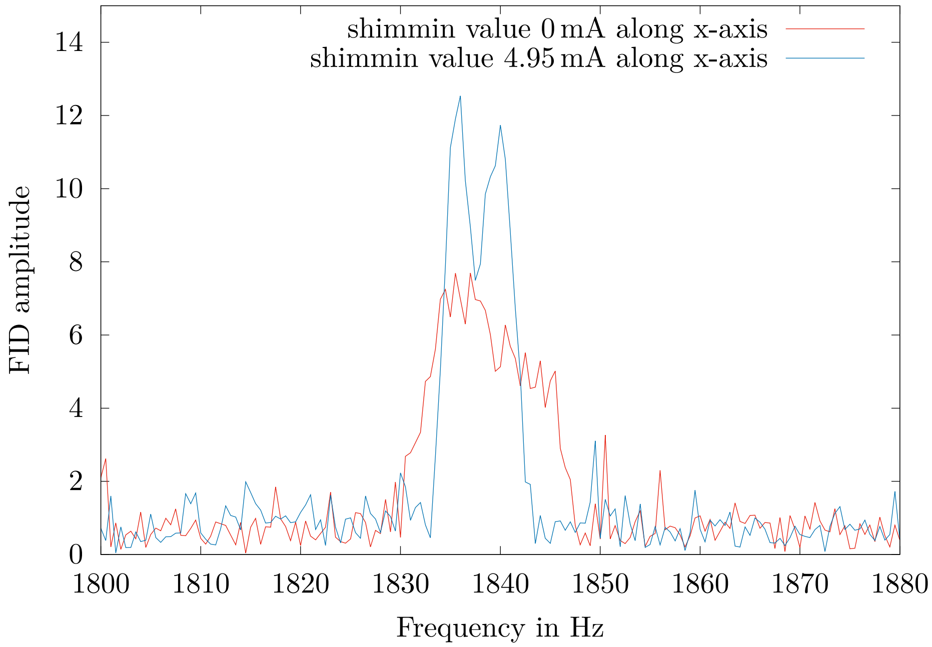


**Figure 7.2:** Spectrum of a single *Hahn* echo applied by different shimming values. Due to more deshimming of the red curve, the apmlitude is lower. Nevertheless the area under the spectrum is the same, due to the same magnetisation.

For the following chapter it is specifcally important to know which relaxation time we observe. Due to the inhomogenious magnetic field there exist different relaxation times of the transversal relaxation time $T_2$. The transversal relaxation time $T_2^*$ describes the relaxation in consideration of the inhomogenious magentic field. Therefore the formula has following shape:

$$\frac{1}{T_2^*} = \frac{1}{T_2} + \gamma \Delta B_0 \; . \tag{7.1}$$

In this equation $\gamma$ is the gyromagnetic ratio of the probe and $\Delta B_0$ is the difference of the magnetic field to its equilibrium. Knowing that we now know that every time we deshimm the system we observe $T_2^*$ and not $T_2$.

# 8 Multiple echo sequences

Beside the *Hahn* echo it is also possible to apply multiple *Hahn* echos in one experimental measurement. This method is called *Call-Purcell-Meiboom-Gill*-method (CPMG). Therefore the 180° pulse is applied every $2\tau$ and thus there accur many maximums in the signal every $2\tau$. The reason to use the CPMG method is that it is possible to measure the amplitude of two consecutiv maxima more often and therefore the measurement of $T_2$ is more precise. More about this will be discussed in the next chapter.

To make the CPMG signals smoother in the time domain we do not use rectangular functions for the pulses, but smoothen them at the edge by a sine-bell-square function. This is possible, due to the fact that it does not change the physical properties of our measurements, but will make them smoother.

A main advantage of CMPG is that errors in the refocusing pulse can be vanished (minimize term of inhomogenious magnetic field), by changing the phase between the $B_1$ excitation and the refocusing pulses. The program *Prospa* profides a function called "Constant 180 pulse phase". This function keeps all the phases of the refocusing pulses equal. The second function *Prospa* provides is "Alternating 180 pulse phase". This function compensates echo errors by alternating the refocusing pulses by 180°. In figure 8.1 it is visible what a change in the 180 pulse phase does to the signal. Unfortunately we only saved the signal vor 180 pulse phases of 270° and 90°. For those two values the signal does not change. That is also the reason why there is only one signal visible. The other one is just directly behind the other one and therefore not visible. If we would have saved a pulse phase of 180° the signal should change to na zu was sollte es sich ändern?? schwächer?, was macht pulse phase eig genau.

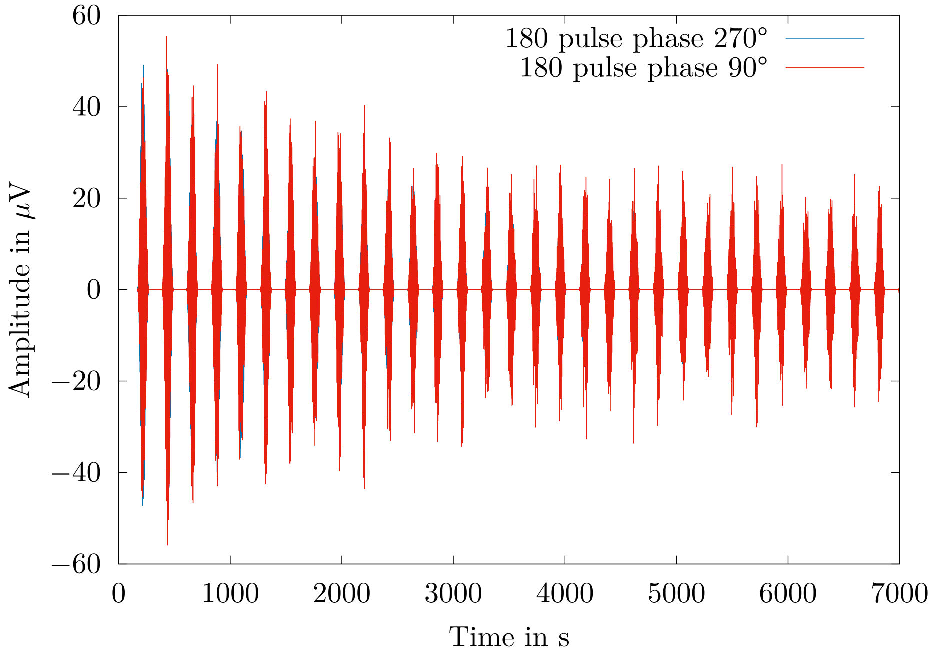


**Figure 8.1:** This figure shows the impact of the 180 pulse phase. Unfortunately we only saved data for a 180 pulse phase of 270° and 90° and for those values it is correct that the signal does not change, but a signal for a 180 pulse phase of 180° would have shown a different signal.

# 9 Transversal relaxation measurements

The last chapter in the first part of this experiment is the transversal relaxation measurement. In order to do so there are two possible ways again.
The first one is by one single *Hahn* echo (spin echo). Therefore the ratio between the maximum of the signal after the 90° pulse and the maximum after the echo (maximum after $2\tau$) provides the transversal relaxation time $T_2$. Figure 9.1 shows measurements for this method by different echo time steps of $2 \cdot 400\,\text{ms}$. The exponential decay is clearly visible, due to the already explained loss ofphase coherence between the spins. Therefore the fit of the datapoints the following formula has been used:

$$M(x) = M_0 \cdot exp(\frac{-x}{T_2}) \ . \tag{9.1}$$

This formula shows a $T_2$ relaxation time of 2691(12) ms. Remember that the phase coherence loss because of the spin spin relaxation is irreversible and is always obtained when measuring $T_2$.

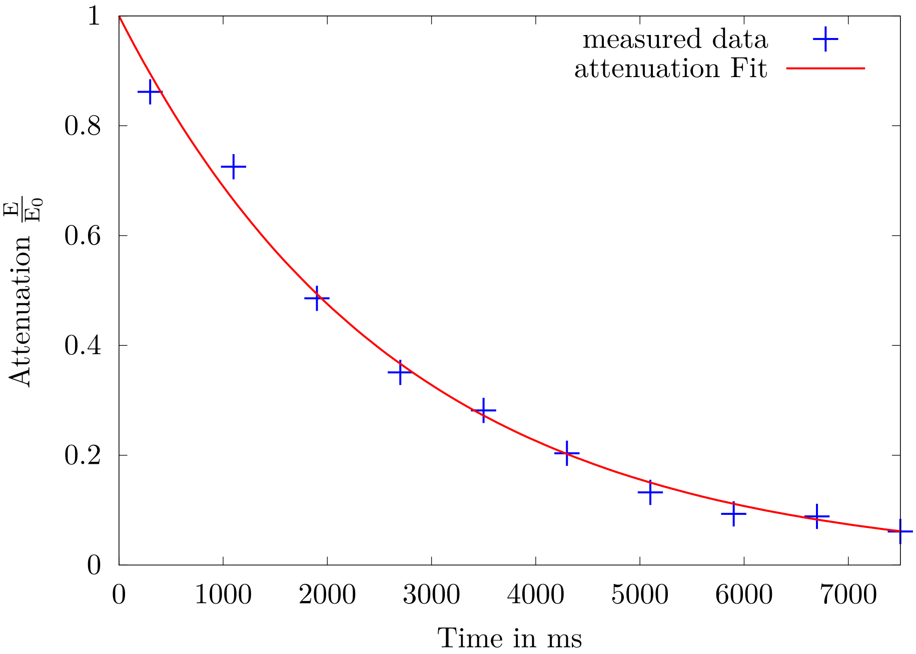


**Figure 9.1:** Attenuation $\frac{E}{E_0}$ for different echo times and exponential fit. The applied exponential fit results in a value for $T_2$ of 2691(12) ms.

One disadvantage of the $T_2$ measurement via one single *Hahn* echo is that the ratio of to back to back maxima is not that exact. Therefore the second option to measure $T_2$ is by using CPMG. Now that more maximums can be observed, the ratio of back to back maxima can be calculated more precisely. Therefore the result of $T_2$ is more exact using this method. Figure 9.2 shows measured data for 30 different echos. Due to the exponential decay the formula 9.1 has been used again to fit the measured data. This results a value for $T_2$ of 2317.760 00(62) ms.

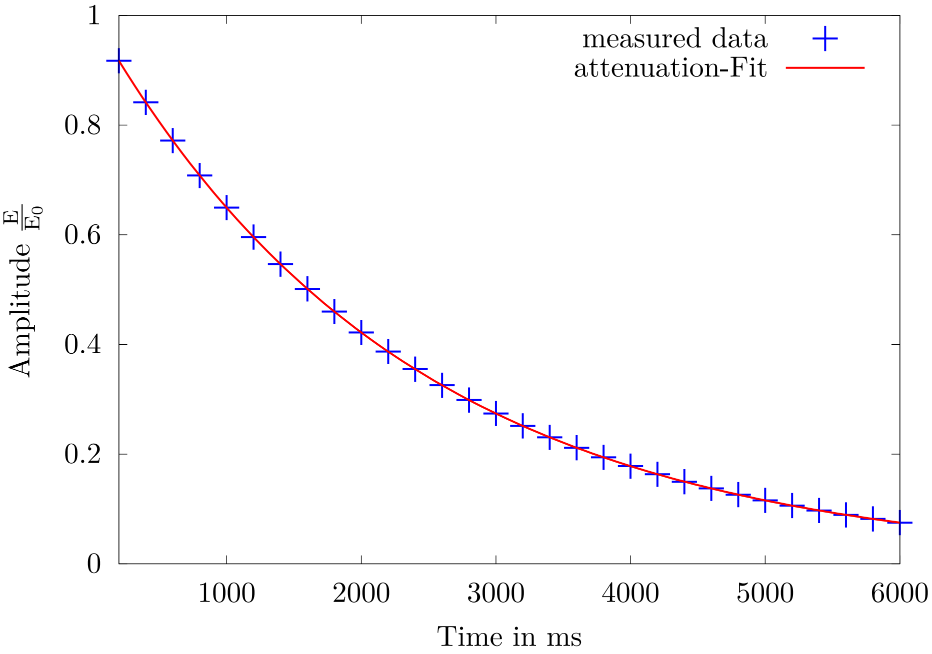


**Figure 9.2:** Attenuation $\frac{E}{E_0}$ for different echo maxima provided by the CPMG method. The applied exponential fit results in a value for $T_2$ of 2317.760 00(62) ms.

The difference of the two $T_2$ values might occur, due to deshimming the system for the CPMG method and therefore can always be some inaccurate pulse phases. Nevertheless note that the CPMG method is the more exact method to measure $T_2$, due to more back to back maxima. By measuring $T_2$ via the *Hahn* echo the inhomogeneity of the magnetic field is reversed, due to the 180° pulses.

# 10 Error discussion and conclusion

## References

[Mor01] Mortazavi, Saideh Sadat: *Earth Field Magnetic Resonance Imaging And Paramagnetic Contrast Agents*, last update: 2009-01-01. https://scholarworks.utep.edu/cgi/viewcontent.cgi?article=3739&context=open_etd, looked up: 2020-07-16.

## List of Figures



## List of Tables

## Attachments